ORIGINAL RESEARCH

Exploration of Potential Therapeutic Targets of Shentong Zhuyu Decoction for Ankylosing Spondylitis Based on Network Pharmacology and Molecular Docking

Haoyang Xin[1],*, Man Wang[2],*, Shuo Wang[3], Haiyan Han[3], Nan Jiang[1]

[1]Department of Nephrology and Rheumatology, Second Affiliated Hospital of Tianjin University of TCM, Tianjin, People's Republic of China; [2]Department of Pharmacy, Tianjin Forth Central Hospital, Tianjin, People's Republic of China; [3]Graduate School, Tianjin University of Traditional Chinese Medicine, Tianjin, People's Republic of China

*These authors contributed equally to this work

Correspondence: Nan Jiang, Department of Nephrology and Rheumatology, Second Affiliated Hospital of Tianjin University of TCM, No. 69, Zengchan Street, Hebei District, Tianjin, 300250, People's Republic of China, Tel +86 18622997255, Email jingnan_jn@126.com

Objective: This study aimed to explore the potential active components and therapeutic targets of Shentong Zhuyu Decoction (SZD) in the treatment of ankylosing spondylitis (AS) through network pharmacology and animal experiments.

Methods: Targets for AS and related pathways were obtained by network pharmacology, and the pathways with the best binding affinity in molecular docking were verified by animal experiments.

Results: The network pharmacology analysis found 248 chemical components, 1068 drug targets and 803 AS-related targets in SZD. After intersection targets analysis, 116 common drug–disease targets were obtained, and matrix metalloproteinase-9, nucleotide-binding oligomerization domain (NOD)-like receptor thermal protein domain associated protein 3 (NLRP3) and cytochrome P450 2D6 were identified as the key targets of SZD for the treatment of AS. A total of 2152 biological processes, 38 cellular component expressions and 150 molecular function terms were obtained in gene ontology enrichment analysis, and 153 Kyoto Encyclopedia of Genes and Genomes (KEGG) signalling pathways were obtained in KEGG enrichment analysis. Molecular docking analysis showed that the absolute binding energies of glypallichalcone and NLRP3, quercetin and NLRP3 and kaempferol and NLRP3 were >7. Animal experiments showed that the expressions of NLRP3, Caspase-1, interleukin (IL)-1β and IL-18 were significantly increased in the model group and the treatment group compared with those in the blank group, and the expression levels in the treatment group were significantly decreased compared with those in the model group ($p < 0.05$).

Conclusion: The active components in SZD, such as baicalin, quercetin, kaempferol and glypallichalcone, may reduce the expression of IL-1β and IL-18 via the NLRP3/Caspase-1 signalling pathway to inhibit the development and progression of inflammation and play a role in the treatment of AS.

Keywords: Shentong Zhuyu Decoction, ankylosing spondylitis, network pharmacology, mechanism of action

Introduction

Ankylosing spondylitis (AS) is an immune-mediated inflammatory arthritis that primarily affects the axial skeleton, particularly the sacroiliac and spinal joints, often leading to severe chronic pain and disability.[1] In addition to bones, AS is associated with anatomical and functional abnormalities in the eyes, skin, gastrointestinal tract, heart and blood vessels.[2] The incidence of AS is closely related to genetics, dyslipidemia and a high ratio of low-density lipoprotein to high-density lipoprotein.[3,4] The incidence of AS in adults is 0.9%–1.4%.[5] Epidemiological studies have found that the incidence of AS in China is approximately 0.3%[6] and is more common in men than in women, with a male-to-female patient ratio of approximately 3:1.[7] No radical treatment options for this disease are currently available, and the main

goal of treatment is to control the clinical symptoms of patients, delay the progression development of the disease, reduce the development of complications and try to maintain the normal morphology of the spine.

Western medicines available for AS mainly include disease-modifying antirheumatic drugs (DMARDs), nonsteroidal anti-inflammatory drugs (NSAIDs), glucocorticoids and biologics.[2] Nonsteroidal anti-inflammatory drugs are the first choice for the treatment of AS. They can significantly relieve symptoms, such as pain and morning stiffness, but cannot prevent the progression of this disease. The long-term use of NSAIDs may lead to gastrointestinal adverse reactions and liver and kidney dysfunction.[8,9] The DMARDs currently used in clinical practice include methotrexate and sulfasalazine, which can effectively improve the condition of patients.[10] However, Zochling et al[11] found that there is no definite evidence to support the effectiveness of DMARDs in the treatment of axial diseases in patients with AS. Biologics are widely used in the treatment of AS due to their potent anti-inflammatory and immunosuppressive effects. However, they are expensive and may aggravate the condition once discontinued.[12] Therefore, traditional Chinese medicine (TCM) has become an area of research due to its unique advantages.

There is no such term as ankylosing spondylitis' in TCM, and instead, this disease is classified into the categories of 'heumatism' and 'dyphosis'. In Neijing, it is stated that 'the kidney is a solitary organ. Yin water of single kidney cannot overcome the Yang fire of the heart and liver, so individuals don't tremble although it is cold. This disease is named heumatism', which is the earliest record of this disease. Heumatism, with an onset location in the bone, is clinically manifested by aching limbs and joints with swelling and even spastic flexion and deformed ankylosis in those with severe conditions.[13] In TCM, it is believed that this disease belongs to the syndrome of deficiency in origin and excess in superficiality, with the kidney and Du meridian deficiency as the root cause and contracting external evil as the symptoms.[14] Retention of wind, cold and dampness in the joints and bones may lead to insufficiency of yang-qi, endogenous blood stasis, phlegm and stasis obstruction of blood vessels.[15] Treatment should be based on the principle of 'treating both symptoms and root causes of the disease'. Traditional Chinese medicine is extensive and profound. There were records of Shentong Zhuyu Decoction (SZD) in the treatment of AS long ago in China.[16] Wang Qingren's SZD[17] drug components mainly include Ligusticum chuanxiong hort, Angelica sinensis, Glycyrrhiza uralensis Fisch, carthamus tinctorius l, Myrrha, Achyranthes bidentata Blume, Notopterygium incisum Ting ex H. T. Chang, Gentiana macrophμlla Pall, Prunus persica (L.) Batsch, Cyperus rotundus, Earthworm, Trogopterori Faeces. This prescription uses Chuanxiong, angelica, peach kernel, safflower to promote blood circulation and remove blood stasis; achyranthes bidentata, Faeces Trogopterori, Earthworm blood Shuluo, Tongbizhitong; qinjiao, Qianghuo Qufeng for dehumidification; xiangfu Xingqi Huoxue and licorice to reconcile the various drugs; it plays the role of relieving pain, dispelling wind and removing dampness, promoting blood circulation and removing blood stasis. Shentong Zhuyu Decoction is effective in promoting qi and relieving pain, reducing inflammation and swelling, promoting blood circulation and resolving blood stasis, which is beneficial to joint pain and lesion recovery.[16]

Network pharmacology (NP) is a new discipline. In NP, a drug–active component–disease–target network is constructed on the molecular level through data visualisation analysis to predict the mechanism of drug treatment for diseases, which makes up for the deficiencies of the "one component, one target, one drug and one disease" paradigm. However, the results of NP need to be validated through corresponding animal experiments to ensure the reliability of these findings. Therefore, the present study was designed to explore the key targets and signalling pathways of SZD in the treatment of AS based on modern pharmacology and data mining. In addition, the findings obtained from NP were verified in animal experiments to reveal the molecular mechanism of this prescription, providing a basis for its clinical use in the treatment of AS.

Materials and Methods
Network Pharmacology
Prediction of the Components and Related Targets of Shentong Zhuyu Decoction
The SZD consisted of 12 traditional Chinese medicinal materials, including Gentiana macrophylla, Ligusticum wallichii, peach kernel, safflower, licorice, notopterygium root, myrrh, Angelica sinensis, Trogopterus dung, Cyperus rotundus, Achyranthes bidentata and earthworm. These materials were searched on the Traditional Chinese Medicine System

Pharmacology Database and Analysis Platform (TCMSP, http://tcmspw.com/tcmsp.php), and all active components were screened based on pharmacokinetic parameters, with an oral bioavailability ≥30 and a drug-likeness ≥0.18 as selection criteria. For those not included in the TCMSP, potential active components were searched in the Traditional Chinese Medicine Integrated Database (TCMID, http://119.3.41.228:8000/tcmid/). The structure of these components was obtained using the PubChem database (https://pubchem.ncbi.nlm.nih.gov/) and imported into the Swiss Target Prediction database (http://www.swisstargetprediction.ch/). Targets with a predicted score >0 were selected as the drug targets.

Acquisition of Disease Targets for Ankylosing Spondylitis

Related targets for AS were searched in the gene-disease and variant-disease association database (DisGeNET, https://www.disgenet.org/) and human gene database (https://www. gene cards.org/, GeneCards) using "ankylosing spondylitis (AS)" as the keyword and used as the potential targets of SZD for the treatment of AS.

This study was conducted in accordance with the Declaration of Helsinki and approved by the Ethics Committee of Second Affiliated Hospital of Tianjin University of TCM.

Construction of Drug–Disease Intersection Targets, Venn Diagrams and Active Component–Target Diagrams

Drug–disease intersection targets were obtained using Venn 2.1.0 (https://bioinfogp.cnb.csic.es/tools/venny/) on the online platform. The active component-related targets of SZD and diseased targets of AS were imported into the Venny 2.1.0 online tool to obtain the drug–disease intersection targets and their Venn diagrams. These intersection targets and active components were then imported into Cytoscape 3.6.1 software (https://cytoscape.org/) to map the drug active component targets to the disease-related targets and construct an active component–target network, with active components and targets denoted by "nodes" and the interrelationships between nodes denoted by "edges".

Construction of the Protein–Protein Interaction Network

The disease-related genes and drug–target intersection genes obtained above were imported into the Search Tool for the Retrieval of Interacting Genes/Proteins (STRING) database (https://string-preview.org/) with the organism set to "Homo Sapiens". The minimum interaction score was set to 0.7, and the free nodes were hidden with system default values for other parameters to obtain the protein–protein interaction (PPI) network for disease–drug intersection genes. These PPI network data were then exported. Using the CytoNCA plugin in Cytoscape 3.8.0 software, computational analysis was conducted based on six parameters, namely betweenness centralities, closeness centralities, degree centralities, eigenvector centralities, local average connectivity-based method centralities and network centralities. Items were retained only when the six parameters were greater than their median values (otherwise, they were deleted) to obtain the core gene network.

Gene Ontology and Kyoto Encyclopedia of Genes and Genomes Analysis

The R software platform and the org.Hs.eg.db package were used to annotate the gene IDs of the disease and drug target intersection genes. After obtaining the gene IDs, R packages, such as "clusterProfiler", "org.Hs.eg.db", "enrich plot" and "ggplot2", were used to perform gene ontology (GO) and Kyoto Encyclopedia of Genes and Genomes (KEGG) analysis for the intersection genes. The GO analysis included three domains: biological process, cellular components and molecular functions. The screening and filtering were conducted with a p-value cutoff of 0.05 and a q-value cutoff of 0.05. The top 10 results of the GO analysis and the top 20 results of the KEGG enrichment analysis were presented in bar charts.

Molecular Docking

Based on the results obtained above, the three active components with the highest numbers of targets were selected as ligands, and the three targets with the highest scores in the core gene network of the PPI network were selected as receptors to perform molecular docking, and the binding energies between them were calculated. A higher absolute value of binding energy suggested a better binding affinity between the ligand and the receptor. The ligands and receptors with the highest binding energies were selected for molecular docking. First, the 3D structure of the active component was searched and downloaded from PubChem (https://pubchem.ncbi.nlm.nih.gov/) using "cnidilin", "glypallichalcone", "GA120", "lico-chalcone a", "xanthinin", "baicalein", "quercetin", "medicarpin", "kaempferol" and "DFV" as keywords. Autodock tools were used to add hydrogen atoms, assign charges to the active components and define the rotatable bonds. Next, the

corresponding protein structures were downloaded from the Research Collaboratory for Structural Bioinformatics Protein Data Bank website (https://www.rcsb.org/) using "MMP9", "NLRP3" and "CYP2D6" as keywords. Pymol software was used to remove the ligands and water molecules in the protein structures, and Autodock tools were used to add hydrogen atoms and assign charges to these proteins. The docking box was set, and Vina was used for molecular docking, with "exhaustiveness" set to 30 and other parameters set as default. The binding energies were calculated. Finally, structure processing and visualisation of the results of molecular docking were conducted using Pymol.

Animal Experiments
Animal Grouping and Modelling
Eighteen 8-week-old female BALB/c mice, SPF grade, weighing 18–21 g, were purchased from Speuf (Beijing) Biotechnology Co., Ltd. The mice were randomly divided into blank group, model group and traditional Chinese medicine group, with 6 mice in each group. Except for the blank group, the other two groups were induced by proteoglycan method:[17] proteoglycan dry powder (Sigma company) was dissolved with 1XPBS (concentration of 2mg/mL), emulsified with complete Freund's adjuvant (Sigma company of the United States) in a ratio of 1:1, 0.1mL of proteoglycan emulsion was injected intraperitoneally, 7 days after the first immunization was carried out for booster immunization, and 0.1mL of emulsion was injected intraperitoneally again, and the modeling process was 21 days in total.

Preparation and Administration of Shentong Zhuyu Decoction
According to the compatibility ratio of the original prescription of "Medical Forest Correction", the prescription of body pain and stasis decoction is as follows: 6g of gentiana macrophylla, 12g of ligusticum wallichii, 18g of peach kernel, 18g of safflower, 12g of licorice, 6g of notopterygium root, 12g of myrrh, 18g of angelica sinensis, 12g of trogopterus dung, 6g of cyperus rotundus, 18g of achyranthes bidentata, 12g of earthworm (to soil).

Source of medicine: one-time purchase from the Chinese medicine pharmacy of the Second Affiliated Hospital of Tianjin University of Traditional Chinese Medicine. The dosage was calculated with reference to the "Equivalent Dose Ratio Table for Humans and Animals by Body Surface Area" in the "Pharmacological Experimental Methodology",[18] and according to the coefficient between humans (70kg) and mice (20g) was 0.0026, the daily crude drug dose of 20g mice was 0.39g crude drug, that is, the crude drug amount was 19.5g/kg. Starting from the 3rd week, the mice in the traditional Chinese medicine group were given gavage once a day for body pain and stasis decoction, and the mice in the other two groups were given the same volume of normal saline gavage once a day for 4 weeks.

Sample Collection and Laboratory Measurements
(1) Levels of serum interleukin (IL)-1β and IL-18 were determined. Briefly, mice were weighed and fully anaesthetized with 1% pentobarbital sodium in normal saline at a dose of 80 mg/kg. The eyeballs were removed, and approximately 1 mL of blood was extracted and placed in a pro-coagulation tube. The blood samples were centrifuged at 250 g for 10 mins, and the serum was collected and transferred to an EP tube, which was stored at −80°C for use. The levels of serum IL-1β and IL-18 were determined for each group using the enzyme-linked immunosorbent assay (ELISA) method with a mouse IL-1β ELISA kit (Ruixin Biotech, China) for IL-1β and a mouse IL-18 ELISA kit (Ruixin Biotech, China) for IL-18. The test was carried out strictly according to the instructions.

(2) Expression of NLRP3 and Caspase-1 mRNAs in tissue were detected. Briefly, hip articular capsule was ground into powder in liquid nitrogen, and 1mL of Trizol solution was added to every 50–100 mg of tissue and ground. The total volume of the sample was <10% of the volume of the Trizol used. The grinding mixture was placed at room temperature for 5 mins, and then chloroform at 0.2 mL/mL Trizol was added. The centrifuge tube was closed tightly and shaken vigorously by hand for 15 secs. The upper aqueous layer was removed into a new centrifuge tube, isopropanol was added at 0.5 mL/mL Trizol and placed at room temperature for 10 mins. After centrifuging at 12,000 g for 10 mins, the supernatant was discarded, and 75% ethanol was added to at least 1 mL/mL Trizol. The mixture was vortexed and centrifuged at 7500 g at 4°C for 5 mins. The supernatant was carefully discarded and dried at room temperature or vacuum-dried for 5–10 mins. The RNAs obtained were dissolved in water, and, if necessary, placed in a water bath at

55°C–60°C for 10 mins. The RNAs were stored in 70% ethanol at −70°C for mRNA isolation. The expression of NLRP3 and Caspase-1 mRNAs was determined by real-time fluorescence quantitative polymerase chain reaction (qRT-PCR).

Before the qRT-PCR, reverse transcription was performed using Hifair® III 1st Strand cDNA Synthesis SuperMix for qPCR (gDNA digester plus) (Yeasen, Shanghai, China). The ready-to-use premix contained RNase-free ddH$_2$O, 5x gDNA digest Mix and 4x Hifair® III SuperMix plus (the reverse transcription system is in Table 1). The reaction included incubation at 25°C for 5 mins, then at 55°C for 15 mins and finally at 85°C for 15 mins. The reverse transcribed cDNA was stored at −20°C. The final volume of the reaction system was 20 μL.

The cDNA obtained above was used in the qRT-PCR. The primer sequences used in the qRT-PCR were synthesised by Sangon Biotechnology Co., Ltd (Shanghai, China) (Table 2). The qRT-PCR was conducted using a MonAmp™ SYBR® Green qPCR Mix kit, with a reaction system of 20 μL (Table 3).

Statistical Analysis

The SPSS 26.0 statistical software package was used for statistical analysis, and the Kolmogorov–Smirnov method was used for the normality test. Measurement data with normal distribution were presented as mean ± standard deviation, the *t*-test was used for the comparison of mean values between groups, variance analysis was used for the comparison of mean values among groups and the Student–Newman–Keuls method was used for pairwise comparison. A significance level of $\alpha = 0.05$ was used for all tests.

Results
Results of Network Pharmacology Analysis
Chemical Components of Shentong Zhuyu Decoction and Their Predicted Targets

A total of 248 chemical components were obtained from SZD through searching the TCMSP and TCMID databases and literature review, including 7 for Ligusticum wallichii, 2 for Angelica sinensis, 92 for licorice, 22 for safflower, 45 for myrrh, 20 for Achyranthes bidentata, 15 for notopterygium root, 2 for Gentiana macrophylla, 23 for peach kernel, 18 for

Table 1 Reverse Transcription System

Reagents	Volume (μL)
5×gDNA digester Mix	3
Total RNA	1
RNase free water	12
4×Hifair® III SuperMix plus	5

Table 2 QRT PCR Primer Sequence

Primer Name	Sequence (5' to 3')
Mice Nlrp3-F	TCACAACTCGCCCAAGGAGGAA
Mice Nlrp3-R	AAGAGACCACGGCAGAAGCTAG
Mice Caspase 1-F	GGCACATTTCCAGGACTGACTG
Mice Caspase 1-R	GCAAGACGTGTACGAGTGGTTG

Table 3 QRT PCR Reaction System

Reagents	Volume (μL)
MonAmp™ SYBR® Green qPCR Mix	10
Forward and reverse primers Gene primers	2
DNA template	2
RNase Free H$_2$O	6

Table 4 Statistical Table of Basic Information on Traditional Chinese Medicine Components Targets in the Drug Group

Drug Name	Quantity of Ingredients (Pieces)	Predicted Number of Targets (Pieces)
Ligusticum chuanxiong hort	7	349
Angelica sinensis	2	43
Glycyrrhiza uralensis Fisch	92	777
Carthamus tinctorius L	22	421
Myrrha	45	545
Achyranthes bidentata Blume	20	427
Notopterygium incisum Ting ex H. T. Chang	15	359
Gentiana macrophμlla Pall	2	44
Prunus persica (L.) Batsch	23	330
Cyperus rotundus	18	402
Earthworm	6	186
Trogopterori Faeces	23	299
Total	248	1068

Cyperus rotundus, 6 for earthworm and 23 for Trogopterus dung (Table 4). Targets for the chemical components of SZD were predicted using the Swiss Target Prediction database, and 1068 drug-related targets were finally obtained.

Disease Targets for Ankylosing Spondylitis

The DisGeNET and GeneCards databases were searched using the keyword "ankylosing spondylitis", and the disease genes obtained from the two databases were integrated. After duplicates were excluded, 803 AS target genes were obtained.

Venn Diagrams of the Drug–Disease Intersection Targets and Drug Component–Disease–Target Network

A total of 1068 drug component-related targets of SZD and 803 AS disease-related targets were imported into the Venny 2.1 online tool. Intersection analysis found 116 common drug–disease targets, and Venn diagrams were constructed (Figure 1). A total of 248 potential active components in the prescription and 116 drug–disease targets were imported into Cytoscape software, and network diagrams of the "drug–component–target–disease" interaction were plotted after isolated components with no intersection with the targets (Figure 2). Topology analysis on the network diagrams was carried out using Network Analyzer. The degree values represented the number of associations between the component
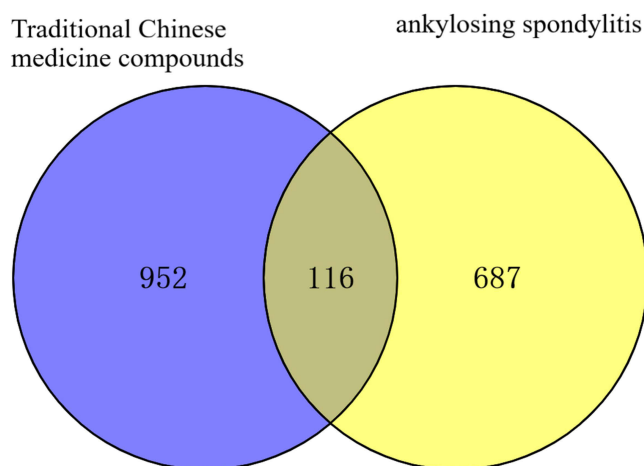
Figure 1 Traditional Chinese medicine compound and target Venn diagram for ankylosing spondylitis.
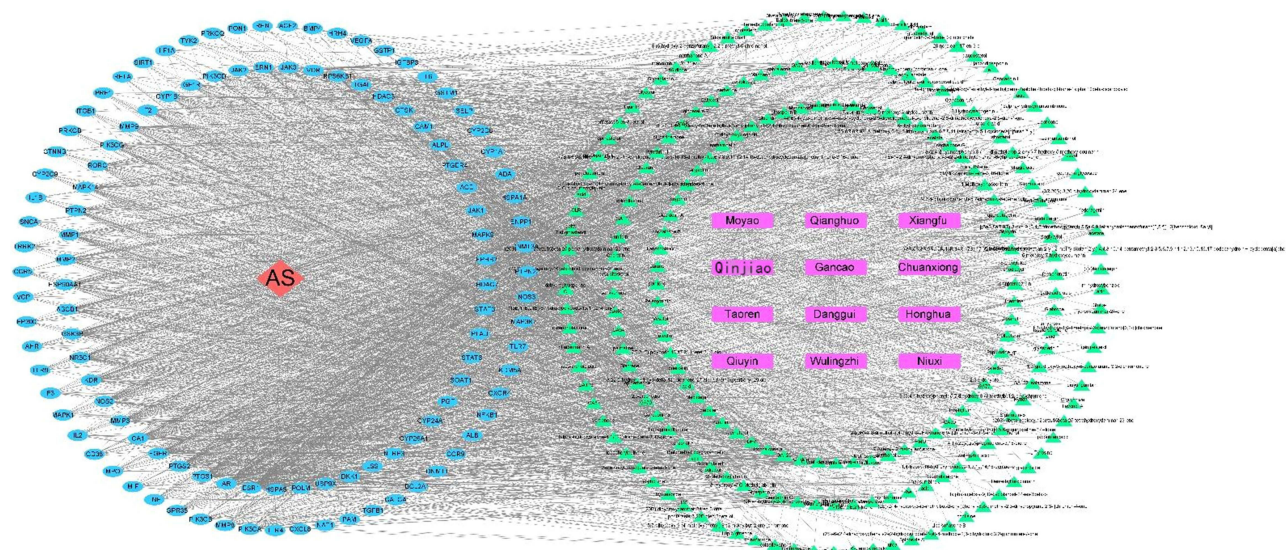
Figure 2 Network diagram of drug component target disease interactions.

and the target, where a higher degree value indicated that the component was more important. The top 10 values of degree for active components are shown in Table 5.

Construction of Protein–Protein Interaction Networks

The 116 common drug–disease targets were imported into the STRING database for searching. The protein type was set to "Homo Sapiens", and the minimum interaction threshold was 0.4 to construct the PPI network (Figure 3). The constructed PPI networks were imported into Cytoscape 3.7.2, and the gene cluster analysis and core target screening were conducted using the MCODE module. A total of three gene clusters (Figure 4) and three core genes, including matrix metalloproteinase-9 (MMP9), NLRP3 and cytochrome P450 2D6, were obtained.

Gene Ontology Functional Enrichment Analysis of the Targets of Shentong Zhuyu Decoction in the Treatment of Ankylosing Spondylitis

A GO analysis of 116 common targets was conducted in three domains using the R program, including the biological process, cellular components and molecular functions. The results of the GO analysis showed the following: the intersection gene set was enriched into 2152 biological pathways, mainly including response to bacterial-derived molecules, response to lipopolysaccharide and regulation of inflammatory responses; the intersection gene set was enriched into 38 cellular component expression processes, mainly including the cytoplasmic vesicle cavity and

Table 5 Main Chemical Components

| Chemical Composition	Degree Value
Cnidilin	24
Glypallichalcone	24
GA120	23
Licochalcone a	22
xanthinin	21
Baicalein	21
quercetin	21
Medicarpin	21
kaempferol	21
DFV	21
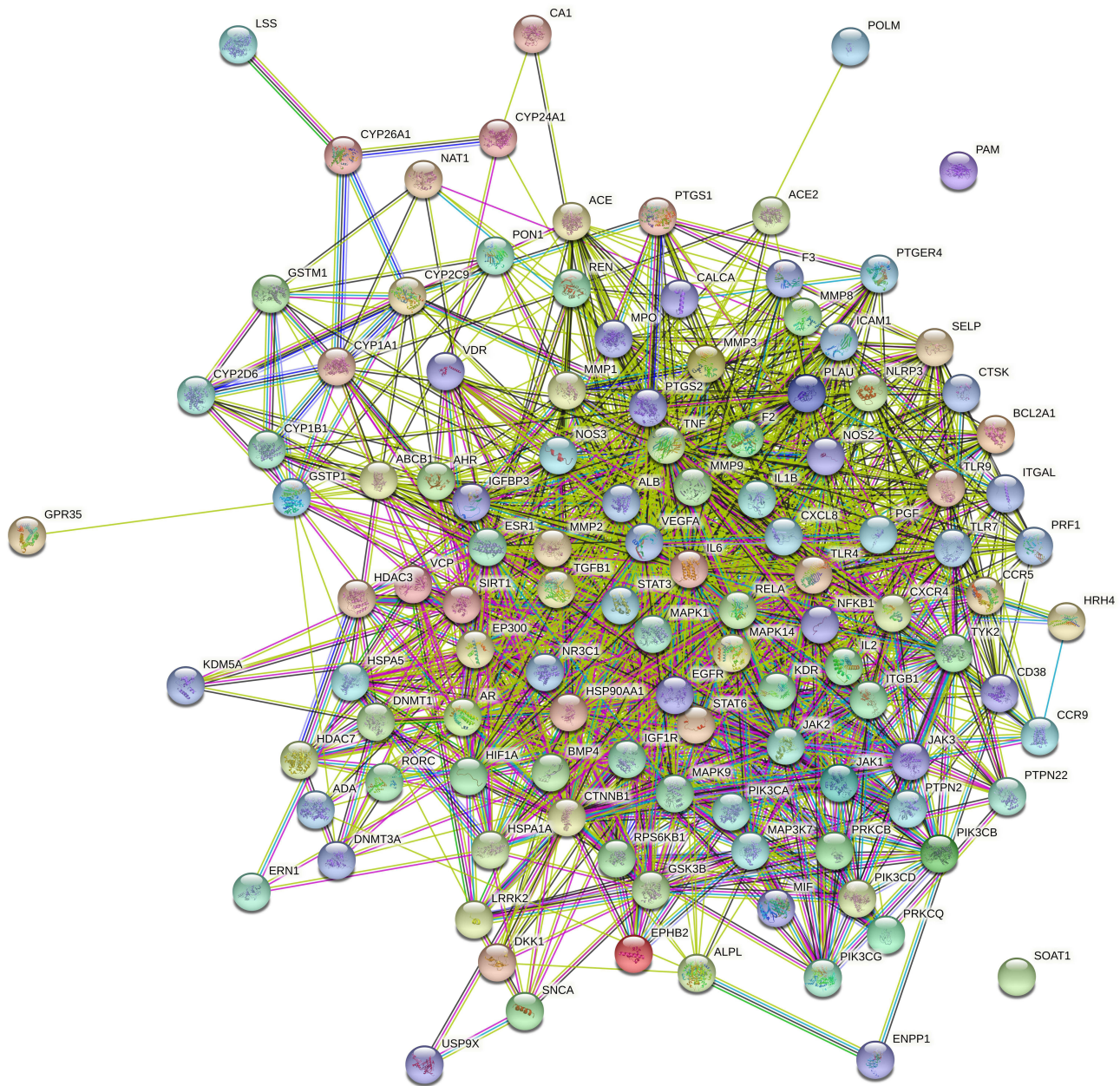
Figure 3 PPI network model diagram.

membrane area; and the intersection gene set was enriched into 150 molecular function related processes, mainly including heme binding and cytokine receptor binding (Figure 5).

Kyoto Encyclopedia of Genes and Genomes Pathway Enrichment Analysis of the Shentong Zhuyu Decoction in the Treatment of Ankylosing Spondylitis

A KEGG analysis of 116 common targets was conducted using the R program, and a total of 153 KEGG pathways were obtained, including PI3K-Akt, Th17 cell differentiation, Toll-like receptors, osteoclast differentiation, JAK-STAT signalling pathway, Th1 and Th2 cell differentiation and platelet activation. The top 20 pathways were compiled into a bar chart of KEGG function enrichment (Figure 6).
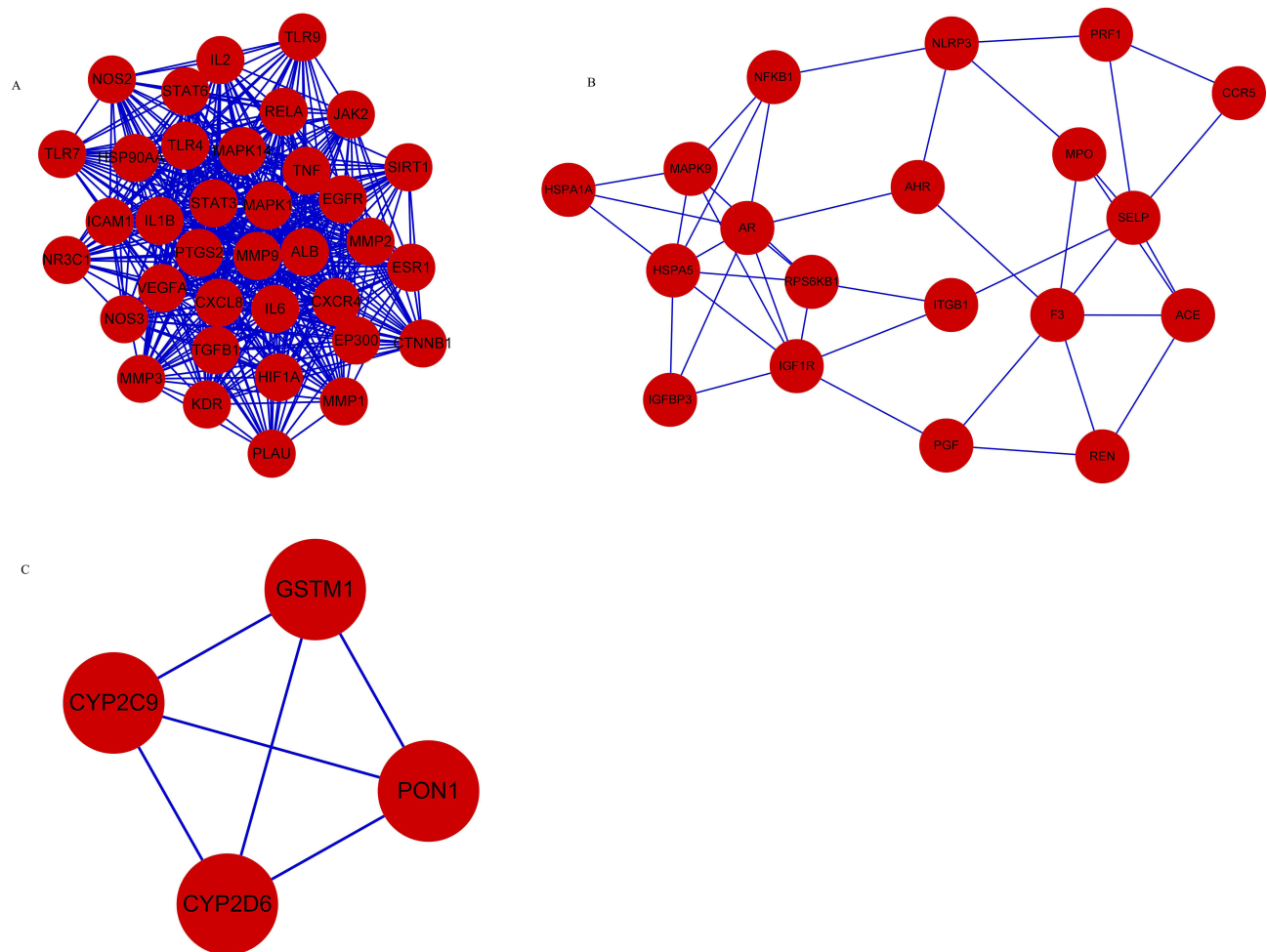
Figure 4 MCODE clustering analysis of gene clusters. (**A**) The core gene network obtained after the first analysis; (**B**) The core gene network obtained after secondary analysis; (**C**) Final Core Gene Network.

Molecular Docking

The binding energies between active components and core genes are shown in Table 6. It was seen that there were three bindings with an absolute binding energy >7, including glypallichalcone and NLRP3, quercetin and NLRP3 and kaempferol and NLRP3. Among them, the best binding affinity was noted between quercetin and NLRP3, with an absolute binding energy of 9.1 kcal/mol. Therefore, the animal experiments below focused on the effect of SZD on the activation of the NLRP3/Caspase-1 pyroptosis signalling pathway and the release of downstream inflammatory factors in AS mice to verify the effectiveness of this regulatory mechanism.

Results of Animal Experiments

Comparison of Nucleotide-Binding Oligomerization Domain-Like Receptor Thermal Protein Domain Associated Protein 3 and Caspase-1 Messenger Ribonucleic Acid Expression Levels in Mouse Tissue Among Groups

Expression levels of NLRP3 and Caspase-1 mRNAs in mouse tissue were determined by qRT-PCR. The amplification and melting curves during the process are shown in Figure 7. The mRNA levels were 1.09 ± 0.23, 8.24 ± 1.55 and 3.66 ± 1.35 ($F = 14.706$, $p < 0.001$) for NLRP3 and 1.05 ± 0.41, 4.58 ± 1.74 and 2.75 ± 0.70 ($F = 78.710$, $p < 0.001$) for Caspase-1 in the blank group, the AS model group and the SZD treatment group, respectively. A further pairwise comparison showed that the expression levels of NLRP3 and Caspase-1 mRNAs in the three groups consistently decreased in the following order: the AS model group > the SZD treatment group > the blank group ($p < 0.05$) (Figure 8).
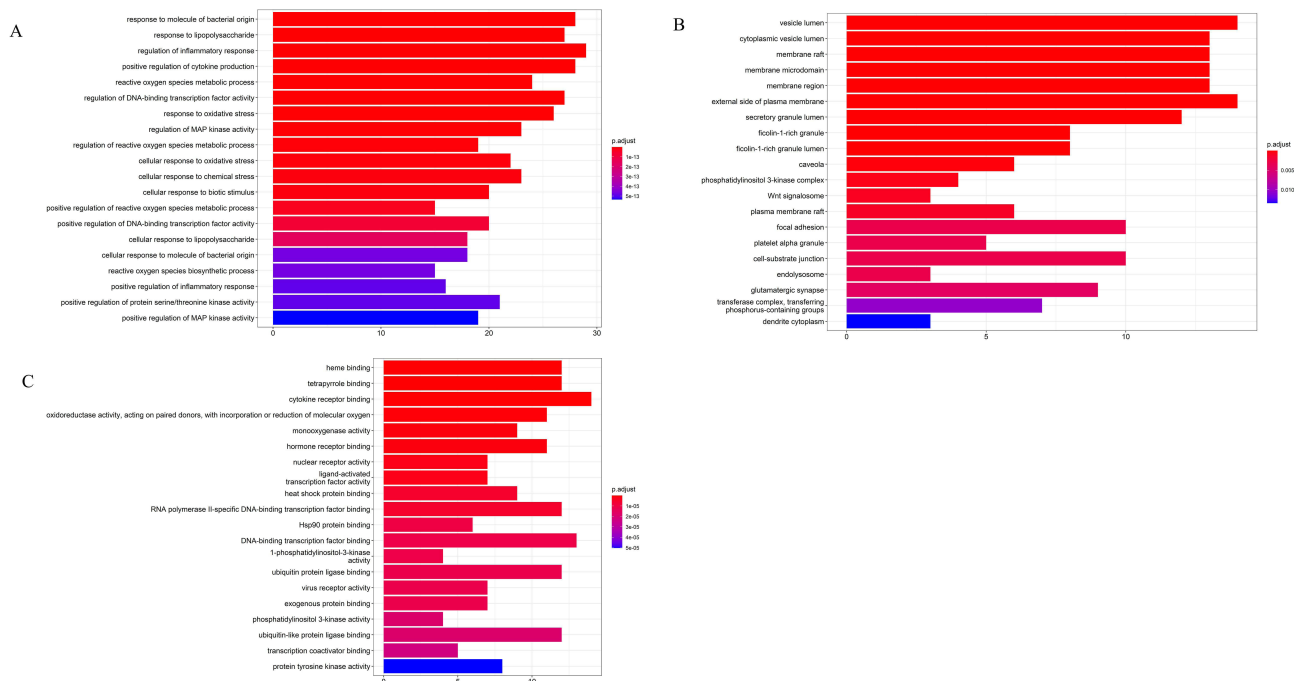
Figure 5 GO enrichment analysis bar chart of traditional Chinese medicine compound in the treatment of ankylosing spondylitis; (**A**) BP.barplot; (**B**) CC.barplot; (**C**) MF. barplot.
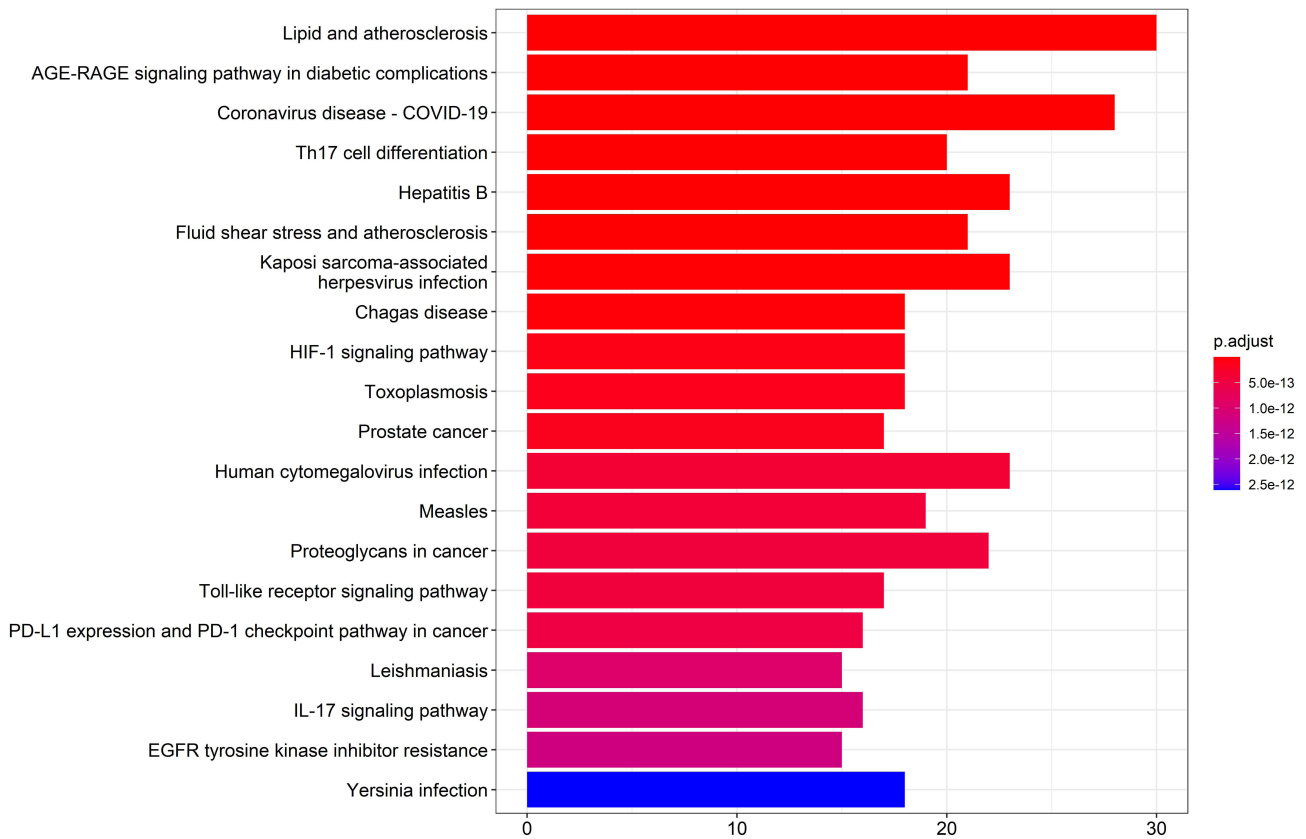
Figure 6 KEGG enrichment analysis of traditional Chinese medicine compound in the treatment of ankylosing spondylitis.

**Table 6** Key Target Docking Results

Ingredients	Target Points	Binding Energy (kcal/mol)
Cnidilin	MMP9	−6.9
	CYP2D6	−6.7
	NLRP3	−5.3
Glypallichalcone	MMP9	−6.1
	CYP2D6	−6.6
	NLRP3	−8.2
GA120	MMP9	−6.5
	CYP2D6	−6.8
	NLRP3	−5.6
Licochalcone a	MMP9	−6.6
	NLRP3	−5.3
	CYP2D6	−5.5
Xanthinin	MMP9	−6.4
	NLRP3	−6.4
	CYP2D6	−5.3
Baicalein	MMP9	−6.4
	CYP2D6	−5.3
	NLRP3	−5.0
Quercetin	MMP9	−5.5
	CYP2D6	−6.4
	NLRP3	−9.1
Medicarpin	MMP9	−5.3
	NLRP3	−5.6
	CYP2D6	−6.1
Kaempferol	MMP9	−5.8
	CYP2D6	−5.8
	NLRP3	−8.9
DFV	MMP9	−5.9
	NLRP3	−5.3
	CYP2D6	−5.7

Comparison of Serum Interleukin-1β and Interleukin-18 Levels Among Groups

The results showed that the serum levels were 67.83 ± 12.42, 111.91 ± 14.21 and 89.72 ± 8.08 ($F = 20.745$, $p < 0.001$) for IL-1β and 19.94 ± 3.16, 40.14 ± 4.94 and 28.78 ± 4.30 ($F = 34.913$, $p < 0.001$) for IL-8 in the blank group, the AS model group and the SZD treatment group, respectively. A further pairwise comparison showed that the levels of serum IL-1β and IL-18 in the three groups consistently decreased in the following order: the AS model group > the SZD treatment group > the blank group ($p < 0.05$) (Figure 9).

Discussion

At present, AS treatment is still in the research stage. Early prevention, detection and treatment are essential to relieve pain and stabilise the condition.[16] Recent studies have shown that biological agents, such as etanercept, have significant clinical efficacy, but their use is limited due to their high price and need for subcutaneous injection. At the same time, with the increase in clinical application, their adverse reactions have been receiving more and more attention, mainly including respiratory tract infections and skin reactions at the injection site. With the inheritance and development of TCM, the progress of TCM foundation and modern research, TCM has provided new ideas for clinical workers to treat AS. In recent years, many experts and scholars have combined experiments and clinical practice. After long-term observation and analysis, they have concluded that TCM can improve the therapeutic effect of patients with AS, particularly in the treatment of integrated traditional Chinese and Western medicine.[13–16,19] Ankylosing spondylitis
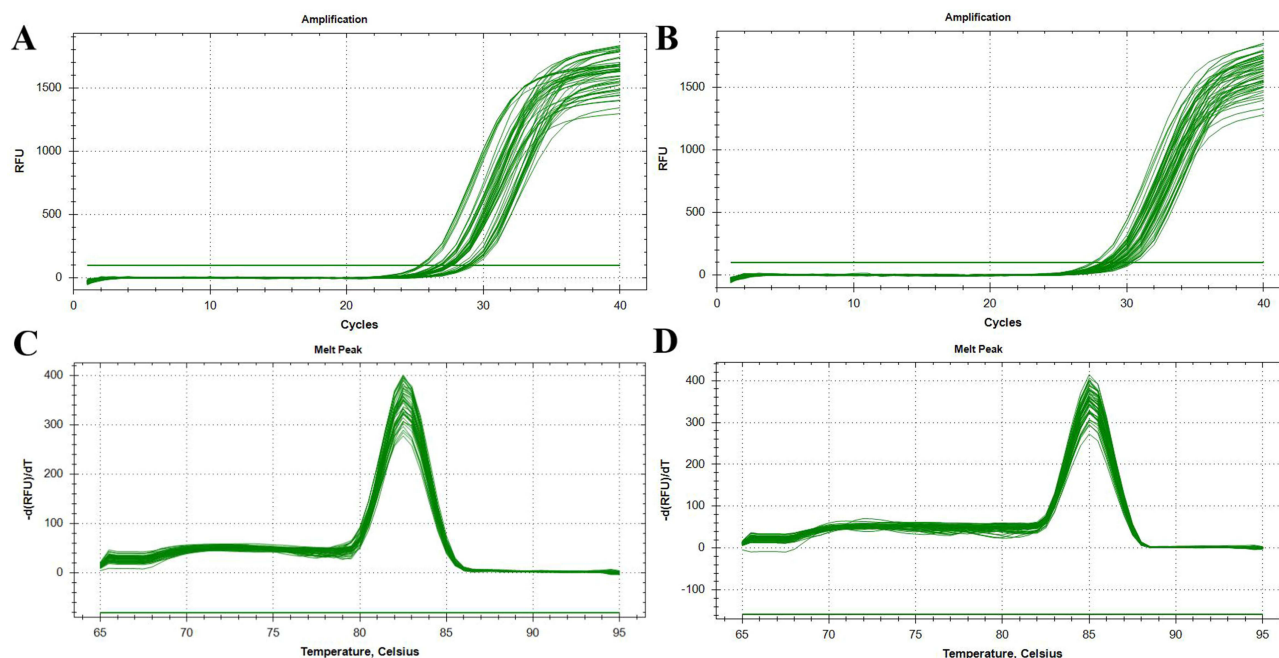
Figure 7 Amplification and dissolution curves during the detection process. (**A**) NLRP3 amplification curve, (**B**) Caspase-1mRNA amplification curve, (**C**) NLRP3 dissolution curve, (**D**) Caspase-1mRNA dissolution curve.
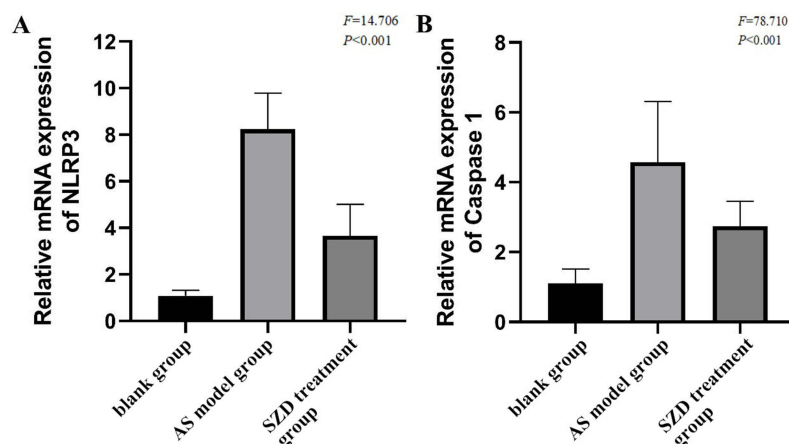
Figure 8 The expression levels of NLRP3 and Caspase-1 mRNA in the tissues of mice in each group, (**A**) NLRP3 expression level, (**B**) Caspase-1 mRNA expression level.

belongs in the categories of "kidney arthralgia" and "bone arthralgia" in TCM. Its treatment principle is mainly to strengthen the body's resistance, eliminate pathogenic factors, promote blood circulation and remove blood stasis. The pathogenesis of AS involves kidney and Du meridian deficiency, yang qi insufficiency and external wind, cold and dampness invasion, which retain in the muscles, bones and joints and lead to obstructed arteries and veins by internal phlegm and blood stasis.[14,15] Shentong Zhuyu Decoction is effective in promoting qi and relieving pain, reducing inflammation and swelling, promoting blood circulation and resolving blood stasis, which is beneficial to joint pain and lesion recovery.[20] In the present study, the active components of the 12 TCM materials in SZD were screened and 248 chemical components were discovered. Furthermore, 1068 drug targets were identified. The main pharmacological components of this prescription included isocorallin, glypallichalcone, GA120, licochalcone A, xanthin, baicalein, quercetin, medicarpin, kaempferol and diflucortolone valerate (DFV).

The GO enrichment analysis and KEGG pathway enrichment analysis showed that SZD played a role in the development and progression of AS by participating in various biological processes and regulating multiple signalling
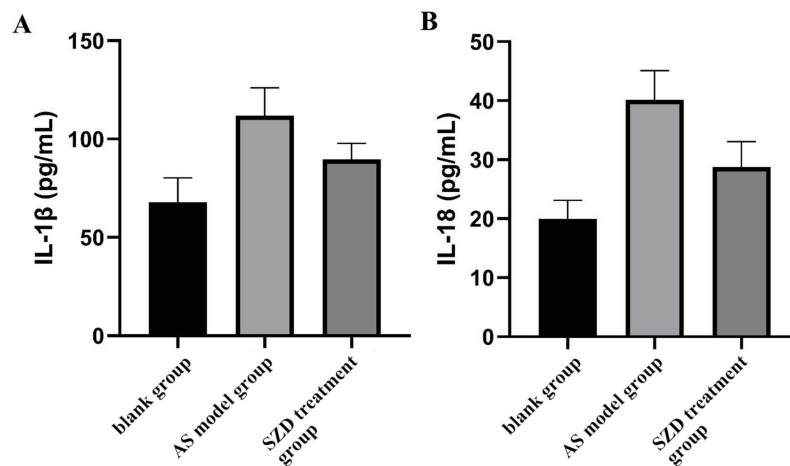
Figure 9 Serum IL-1 in mouse tissues of each group β And IL-18 levels, (**A**) serum IL-1 β Level, (**B**) Serum IL-18 level.

pathways. Atherosclerosis is one of the serious complications caused by the inflammatory factors involving the heart and blood vessels in AS.[21] The development of atherosclerosis in patients with AS may be attributed to the high disease activity and limited functions, and 25(OH)D3 deficiency is one of the risk factors for the accelerated development of atherosclerosis.[22] In addition, increased oxidative stress, elevated serum placental growth factor, soluble CD40 ligand and thickened intima-media also serve as risk factors for accelerated atherosclerosis in male patients with active AS and without typical cardiovascular risk factors.[23] These findings are closely related to the terms found in the GO analysis in the present study, including "response to lipopolysaccharides", "steroid metabolism process", "reactive oxygen species metabolism process" and "response to toxic substances". Regarding these risk factors, studies have found that whole-body cryotherapy can reduce the levels of biomarkers for inflammation, oxidative stress and atherosclerotic plaques and consequently slow down the progression of atherosclerosis in male patients with active AS and without typical cardiovascular factors.[24] Carotid atherosclerosis was significantly reduced in patients with AS treated with tumour necrosis factor (TNF) antagonists compared with the healthy control group, indicating that this treatment plays an important complementary role in reducing the progression of vascular disease; this may be explained by the effects of TNF antagonists on the concentrations of oxidised low-density lipoprotein, β2-glycoprotein I and brain-type natriuretic peptide.[25,26] These results are closely related to the "TNF signalling pathway", "NF-kB signalling pathway", and "NOD-like receptor signalling pathway" identified in the enrichment analysis of the KEGG pathway in the present study. As described above, the possible underlying mechanisms of SZD in the treatment of AS include relieving vascular inflammation, softening the vascular walls and unblocking blood vessels to restore normal blood flow velocity (ie the effect of "tonifying qi, warming meridians and harmonising blood and unblocking obstruction"), which reflect the TCM theory that "if there is free flow, there is no pain".

Molecular docking was carried out between the top 10 active components with the highest number of predicted targets and the three genes with the highest scores in the core gene interaction network. Three bindings were found with an absolute binding energy >7, namely glypallichalcone and NLRP3, quercetin and NLRP3 and kaempferol and NLRP3; the best binding affinity was seen between quercetin and NLRP3, with an absolute binding energy of 9.1 kcal/mol. Therefore, animal experiments were further conducted to explore and validate the mechanism of glypallichalcone, quercetin and kaempferol in inhibiting the development of AS via the NLRP3/Caspase-1 pathway.

Ankylosing spondylitis is related to pyroptosis. Pyroptosis, also known as inflammatory cell death, is a significant inflammatory response induced by cell swelling, cell rupture and release of cytoplasmic contents due to the formation of cell membrane micropores.[27] The inhibition of NLRP3 inflammasome activation can prevent the occurrence of pyroptosis, and activation of NLRP3 inflammasome induces pyroptosis. When pyroptosis occurs, the cell membrane swells and breaks,[28] and the cellular contents, including inflammatory cytokines IL-1β and IL-18,[29] are released into the extracellular space. In addition, pyroptosis is Caspase-1-dependent,[30] and the expression of caspase-1 significantly

increases during pyroptosis.[31] Baicalin, kaempferol and quercetin belong to flavonoids. Studies have shown that flavonoids can inhibit the release of IL-1β and IL-18 via the NLRP3/Caspase-1 pathway by enhancing cAMP-PKA signalling to prevent pyroptosis. Recent studies[32] have found that glypallichalcone is a potential antioxidant and anti-inflammatory agent and is being widely investigated by researchers. Autophagy and activation of inflammasome are two basic cellular responses to external stimuli. Some studies[33] have shown that autophagy and inflammation interact with each other and maintain a dynamic balance under various stresses. Furthermore, some studies[34] have confirmed that glypallichalcone can reduce inflammatory damage by promoting autophagy and mediating the inactivation of NLRP3 inflammasome. The results of animal experiments in the present study also demonstrated that the levels of NLRP3, Caspase-1, IL-1β and IL-18 in the SZD treatment group were decreased compared with those in the AS model group, which were consistent with the findings described above. These results indicated that SZD inhibited the development and progression of inflammation by downregulating the levels of IL-1β and IL-18 via the NLRP3/Caspase-1 pathway.

There were some limitations in the present study. First, these are representatives of important active components of SZC identified by the NP method, which cannot completely replace the efficacy of the prescription itself. Further in vitro cell experiments are needed to confirm this mechanism. Second, investigations into the efficacy of SZD in the present study were carried out at the animal experiment level, and further clinical studies are needed.

Conclusion

In summary, the active components of SZD, including baicalin, quercetin, kaempferol and glypallichalcone, may reduce the levels of IL-1β and IL-18 through the NLRP3/Caspase-1 signalling pathway to inhibit the development and progression of inflammation and play a role in the treatment of AS, providing a molecular basis for further studies of TCM in the treatment of this disease.

Data Sharing Statement

All data generated or analyzed during this study are included in this published article.

Ethics Approval and Consent to Participate

This study was conducted in accordance with the Declaration of Helsinki and approved by the Ethics Committee of Second Affiliated Hospital of Tianjin University of TCM. All laboratory operations on Animals followed the Guidelines for the Care and Use of Laboratory Animals, and the study was approved by the Animal Ethical and Welfare Committee of Institute of Radiation Medicine, Chinese Academy of Medical Sciences.

Acknowledgments

Funding

Disclosure

None of the authors have any personal, financial, commercial, or academic conflicts of interest to report for this work.

References

1. Voruganti A, Bowness P. New developments in our understanding of ankylosing spondylitis pathogenesis. *Immunology*. 2020;161(2):94–102. doi:10.1111/imm.13242
2. Daikh DI, Chen PP. Advances in managing ankylosing spondylitis. *F1000Prime Rep*. 2014;6:78. doi:10.12703/P6-78
3. Hanson A, Brown MA. Genetics and the Causes of Ankylosing Spondylitis. *Rheum Dis Clin North Am*. 2017;43(3):401–414. doi:10.1016/j.rdc.2017.04.006
4. Berg IJ, Semb AG, van der Heijde D, et al. CRP and ASDAS are associated with future elevated arterial stiffness, a risk marker of cardiovascular disease, in patients with ankylosing spondylitis: results after 5-year follow-up. *Ann Rheum Dis*. 2015;74(8):1562–1566. doi:10.1136/annrheumdis-2014-206773
5. Reveille JD, Witter JP, Weisman MH. Prevalence of axial spondylarthritis in the United States: estimates from a cross-sectional survey. *Arthritis Care Res*. 2012;64(6):905–910. doi:10.1002/acr.21621
6. Dean LE, Jones GT, MacDonald AG, et al. Global prevalence of ankylosing spondylitis. *Rheumatology*. 2014;53(4):650–657. doi:10.1093/rheumatology/ket387
7. Wu SS, Duan ZH, Pan FM. Advances in epidemiology of ankylosing spondylitis. *Acta Univ Med Anhui*. 2013;48(8):988–992.
8. Taurog JD, Chhabra A, Colbert RA. Ankylosing Spondylitis and Axial Spondyloarthritis. *N Engl J Med*. 2016;374(26):2563–2574. doi:10.1056/NEJMra1406182
9. Xing S, Gao YZ, Gao K, et al. Current development and prospect of NSAIDs in the treatment of ankylosing spondylitis. *Rheum Arthritis*. 2015;4(3):60–63,68. doi:10.3969/j.issn.2095-4174.2015.03.017
10. Wang D. Clinical observation on treatment of ankylosing spondylitis of jibi kidney deficiency and du cold syndrome with duhuo jisheng decoction and western medicine. *J Liaoning Univ Traditional Chin Med*. 2020;22(5):95–99. doi:10.13194/j.issn.1673-842x.2020.05.023
11. Zochling J, van der Heijde D, Burgos-Vargas R, et al. ASAS /EULAR recommendations for the management of ankylosing spondylitis. *Ann Rheum Dis*. 2006;65(4):442–452. doi:10.1136/ard.2005.041137
12. Lei JX, Dai L, Huang F, et al. Systematic evaluation of clinical efficacy and safety of bushen qiangdu recipe combined with sulfasalazine for treatment of ankylosing spondylitis. *J Guangzhou Univ Tradit Chin Med*. 2020;37(5):989–995.
13. Li MY, Lou YQ. The origin and relevant historical literature review of bone rheumatism. *Rheum Arthritis*. 2014;3(12):59–68.
14. Zhang GL, Liu J, Xin L, et al. Study on the drug use rule of traditional Chinese medicine in treating ankylosing spondylitis based on 895 hospitalized cases data mining. *J Jiangxi Coll Tradit Chin Med*. 2019;31(3):30–34.
15. Shen Y, Ding HB, Cheng P, et al. Study on classification of traditional Chinese medicine syndromes of 278 ankylosing spondylitis patients. *Shanghai J Traditional Chin Med*. 2020;54(7):34–38. doi:10.16305/j.1007-1334.2020.07.001
16. Gao Y, Zhang Y. Observation on the efficacy of etanercept in the active stage of axial ankylosing spondylitis. *Chinese J Mod Drug App*. 2017;11(19):126–127. doi:10.14164/j.cnki.cn11-5581/r.2017.19.069
17. Xu YY. *The Effect of Kidney Tonifying and Governor Strengthening Treatment Formula on the IL-23/Th17 Axis in an Animal Model of Ankylosing Spondylitis*. Guangzhou University of Traditional Chinese Medicine; 2017.
18. Wei W, Wu XM, Li YJ. *Pharmacological Experimental Methodology*. 4th ed. People's Medical Publishing House; 2010:1698.
19. Huang ZX, Guo XQ, Deng WM, et al. Comparison of the efficacy of different courses of etanercept in the treatment of ankylosing spondylitis. *Clin Med Eng*. 2018;25(04):447–448.
20. Yang JT. Therapeutic effect of Shentong Zhuyu Decoction combined with acupuncture and massage on lumbocrural pain. *Heath Everyone*. 2019;496(11):115–116.
21. Kucuk A, Uğur Uslu A, Icli A, et al. The LDL/HDL ratio and atherosclerosis in ankylosing spondylitis. *Z Rheumatol*. 2017;76(1):58–63. English. doi:10.1007/s00393-016-0092-4
22. Fotoh DS, Serag DM, Badr IT, et al. Prevalence of subclinical carotid atherosclerosis and vitamin D deficiency in Egyptian ankylosing spondylitis patients. *Arch Rheumatol*. 2020;35(3):335–342. doi:10.46497/ArchRheumatol.2020.7694
23. Stanek A, Cholewka A, Wielkoszyński T, et al. Increased levels of oxidative stress markers, soluble CD40 ligand, and carotid intima-media thickness reflect acceleration of atherosclerosis in male patients with ankylosing spondylitis in active phase and without the classical cardiovascular risk factors. *Oxid Med Cell Longev*. 2017;2017:9712536. doi:10.1155/2017/9712536
24. Stanek A, Cholewka A, Wielkoszyński T, et al. Whole-body cryotherapy decreases the levels of inflammatory, oxidative stress, and atherosclerosis plaque markers in male patients with active-phase ankylosing spondylitis in the absence of classical cardiovascular risk factors. *Mediators Inflamm*. 2018;2018:8592532. doi:10.1155/2018/8592532
25. Zardi EM, Pipita ME, Giorgi C, et al. Differences in carotid atherosclerosis between patients with ankylosing spondylitis treated with tumor necrosis factor-α antagonists and healthy matched controls. *Medicine*. 2018;97(27):e11250. doi:10.1097/MD.0000000000011250
26. Pusztai A, Hamar A, Horváth Á, et al. Soluble vascular biomarkers in rheumatoid arthritis and ankylosing spondylitis: effects of 1-year antitumor necrosis factor-α therapy. *J Rheumatol*. 2021;48(6):821–828. doi:10.3899/jrheum.200916
27. Vanden berghe T, Hassannia B, Vandenabeele P. An outline of necrosome triggers. *Cell Mol Life Sci*. 2016;73(11–12):2137–2152. doi:10.1007/s00018-016-2189-y
28. Ding J, Wang K, Liu W, et al. Pore-forming activity and structural autoinhibition of the gasdermin family. *Nature*. 2016;535(7610):111–116. doi:10.1038/nature18590
29. Bai JJ, Long JE. Primary study on molecular characteristics and mechanisms of enterovirus type 71-induced programmed cell death. *J Microbes Infect*. 2018;13(4):198–206. doi:10.3969/j.issn.1673-6184.2018.04.002
30. Shi J, Zhao Y, Wang K, et al. Cleavage of GSDMD by inflammatory caspases determines pyroptotic cell death. *Nature*. 2015;526(7575):660–665. doi:10.1038/nature15514
31. Fricker M, Tolkovsky AM, Borutaite V, et al. Neuronal cell death. *Physiol Rev*. 2018;98(2):813–880. doi:10.1152/physrev.00011.2017
32. Zhong CL, Huang GT, Zhang ZQ. Effect of schisandrin B on pathological injury, inflammatory response, and nuclear factor-kappa B expression in lung tissue of rats with sepsis and acute lung injury induced by lipopolysaccharide. *J Anhui Univ Chin Med*. 2020;39(6):57–62. doi:10.3969/j.issn.2095-7246.2020.06.016

33. Paik S, Kim JK, Silwal P, et al. An update on the regulatory mechanisms of NLRP3 inflammasome activation. *Cell Mol Immunol.* 2021;18 (5):1141–1160. doi:10.1038/s41423-021-00670-3

34. Fan FF, Wang Y, Dong X, et al. Glypallichalcone regulates autophagy and NLRP3 inflammasome to alleviate myocardial injury in sepsis. *J Inner Mongolia Medl Univ.* 2023;45(04):361–365. doi:10.16343/j.cnki.issn.2095-512x